SCIENTIFIC REPORTS

OPEN

SUBJECT AREAS:
FERROELECTRICS AND MULTIFERROICS
SURFACES, INTERFACES AND THIN FILMS

Received
24 June 2014

Accepted
7 October 2014

Published
30 October 2014

Correspondence and requests for materials should be addressed to N.B. (nick.barrett@cea.fr)

Reversible switching of in-plane polarized ferroelectric domains in $BaTiO_3$(001) with very low energy electrons

J. E. Rault[1], T. O. Menteș[2], A. Locatelli[2] & N. Barrett[3]

[1]Synchrotron-SOLEIL, BP 48, Saint-Aubin, F-91192 Gif sur Yvette CEDEX, France, [2]Elettra-Sincrotrone Trieste S.C.p.A.. Strada Statale 14 - km 163, 5 in AREA Science Park 34149 Basovizza, Trieste, Italy, [3]CEA, DSM/IRAMIS/SPEC, F-91191 Gif-sur-Yvette Cedex, France.

The switchable bipolar ground state is at the heart of research into ferroelectrics for future, low-energy electronics. Polarization switching by an applied field is a complex phenomenon which depends on the initial domain ordering, defect concentration, electrical boundary conditions and charge screening. Injected free charge may also to be used to reversibly switch in-plane polarized domains. We show that the interaction between the initial domain order and the bulk screening provided by very low energy electrons switches the polarization without the collateral radiation damage which occurs when employing a beam of high energy electrons. Polarization switching during charge injection adds a new dimension to the multifunctionality of ferroelectric oxides.

One of the fundamental property of ferroelectric (FE) materials is that their spontaneous electric polarization may be reversed under application of an external field. To minimize the electrostatic and elastic energy in a FE, local electric dipoles order, leading to the formation of polarized domains, indeed ferroelectric switching has been shown to be strongly influenced by existing ferroelastic domains[1,2]. In Merz's original theory of domain formation and switching, the application of an electric field gives rise to a transient current due to displacement of the polarization charge[3], one would therefore expect that the injection of free charge might switch the polarization. Electron beams can lead to specimen charging, setting up a potential difference and generating an internal electric field large enough to switch polarization[4].

In- and out-of-plane domains can be switched using 10–30 keV electron beams from a scanning electron microscope[5]. Electron beam irradiation of sub-micron $BaTiO_3$ single crystals in a transmission electron microscope (TEM) has been used to create quadrant domains, originating from the radial field[6] produced by a sufficiently high, local radiation dose[7]. The very high electron energies delivered in TEM can also create defects, particularly oxygen vacancies (V_O). For example, radiation-induced V_O in $LiNbO_3$ enhance ionic diffusion of Li, redefining the domain polarization[8].

However, high energy e-beam polarization switching by radial fields or radiation-induced V_O is generally irreversible. In the first case, reverse switching would require charge of opposite sign, for example, positively charged ions, but with no guarantee of producing the original domain structure. In the second case, radiation-induced oxygen vacancies remain when the beam is turned off, pinning the polarization.

Yakshinskiy *et al.* showed that no oxygen desorption was observed on TiO_2 surface when the electron beam energy is below 20 eV[9]. Thus, very low energy electrons can provide extra charge without inducing V_O. Although there are no reports on low energy e-beam switching in the literature, it represents a challenging and fascinating new potential avenue to manipulate FE polarization with a view to novel bipolar ferroelectric device applications.

High resolution transmission Electron Microscopy (STEM) has been used, for example, to study dipoles at domain walls in $Pb(Zr,Ti)O_3$ with atomic resolution[10,11] or the switching dynamics in a $BiFeO_3$ thin film[12]. Piezo-response Force Microscopy (PFM) has been used to follow nucleation and domain wall motion during switching of ferroelectric films of $Pb(Zr,Ti)O_3$[13] and $BiFeO_3$[14]. However, high energy electron irradiation in the case of TEM or tip-surface contact in the case of PFM can also influence the experimental observations. Low energy electron microscopy is a non-contact low energy imaging technique can provide less invasive, full-field of surface FE

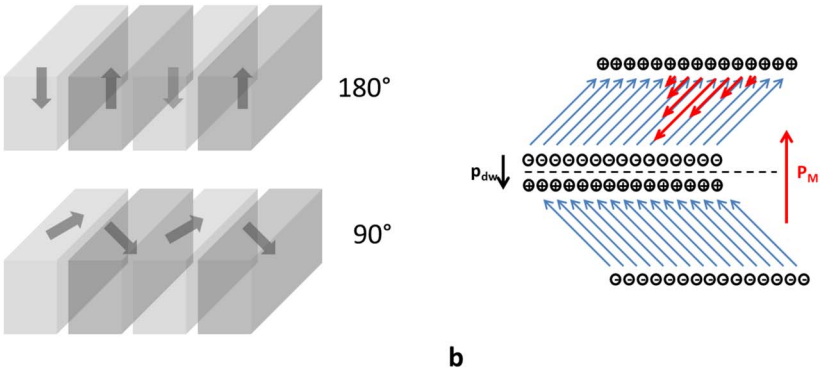

Figure 1 | (a) Schematic of 180° (top) and 90° (bottom) domain walls in $BaTiO_3$(001). In the latter the polarization directions are in-plane (b) 90° domain walls between in-plane polarized domains showing net macroscopic polarization and domain wall dipoles. The thicker (red online) arrows represent the switched polarization in the form of a needle, described below.

domain structures[15]. In this article, we use a low energy electron microscope (LEEM) to simultanously manipulate and observe in-plane FE domains of a $BaTiO_3$ single crystal.

Two types of domain wall can exist in tetragonal $BaTiO_3$, defined by the angle between the polarization in adjacent ferroelectric domains. 180° domain walls separate anti-parallel polarizations and make an angle of 90° with the (001) surface, shown in Fig. 1a. Surface polarization charge gives a distinctive electrical topography which can be directly imaged by low energy electrons[16,17]. On the other hand, 90° domain walls form a boundary between either in- and out-of plane domains, making an angle of 45° with respect to the surface or two in-plane domains, in which case the wall is at 90° with respect to the surface[3]. In-plane domain ordering with 90° domain walls gives rise to a net macroscopic polarization, $\vec{P}_M$, as shown in Fig. 1b. Furthermore, at each domain wall an electric dipole $\vec{p}_{dw}$ is created, opposite in sign to $\vec{P}_M$. 90° domain walls in $BaTiO_3$ also define ferroelastic domains and are a convenient way to reduce strain energy. In films, they have been shown to drive the back-switching of the polarization[1]. As we will demonstrate shortly, the 90° walls between in-plane polarized domains are consistent with the switching patterns observed in this experiment.

Results

Surface preparation and characterization. An optical micrograph of the $BaTiO_3$ single crystal is shown in Fig. 2a. Long range ferroelastic domain ordering is visible, extending over the whole crystal surface[3]. For reference, the diameter (85–90 μm) of the electron beam used in the experiments is shown as the black circle.

The electron microscopy investigations were carried out using a low energy electron microscope. The e-beam was used both for domain manipulation and imaging. It provides a 20 nA electron beam into an elliptical 90 × 85 μm^2 beam spot was used giving an incident flux of 2.1×10^{19} e/(m^2s). At very low electron kinetic energy (KE), called mirror electron microscopy (MEM), electrons are reflected without penetrating the sample surface. At higher KE (LEEM), the electrons penetrate the surface. In between, the reflectivity gives measure of the local work function or surface potential[18].

Ideal ferroelectrics are insulators, however, it has been shown theoretically[19–21] and experimentally[22] that the ferroelectric state can exist up to a critical doping level, making imaging possible with low energy electrons and photoelectrons. We achieve such moderate doping by annealing in ultra-high vacuum, a procedure known to produce oxygen vacancies in a controlled manner[23,24]. Each V_O liberates two electrons which reduce neighboring Ti cations to Ti^{3+}. The diffusion coefficient of oxygen in $BaTiO_3$ is 10^{-11} m^2 s^{-1} (see ref. 25), thus after 2 hours annealing in vacuum we estimate that the V_O concentration extends ~10 μm into the sample, three orders of magnitude greater than the inelastic mean free path of low energy electrons. Thus the entire volume of the $BaTiO_3$ interacting with the incident electron beam is assumed to have a homogeneous V_O concentration. By carrying out microprobe-low energy electron diffraction (μ-LEED) we have acquired LEED images of the $BaTiO_3$ surface, shown in Fig. 2b. The LEED pattern is sharp, corresponding to a (1 × 1) bulk-terminated surface structure. There is a high background in the LEED pattern, which may be due to the presence of disordered oxygen vacancies on the surface. The LEED pattern and the complementary PEEM measurements described in the Supplementary Fig. 2 and 3 demonstrate that the surface is free from reconstruction and significant extrinsic contamination.

Experimentally, the electron KE is controlled by the sample bias or start voltage (SV). Images were collected at 1 and 5 eV SV. At 1 eV (close to MEM) the reflectivity is near to a maximum. At 5 eV the electrons penetrate ~10 nm into the sample[26] giving a charge density of 2.1×10^{27} e/(m^3s), comparable to the 1.56×10^{28} e/m^3 reported by Ahluwalia *et al.*[7]. The net injected charge does not change sign with increasing energy up to few tens of eV, as shown in the Supplementary Fig. 1, however, the change in start voltage from 1 to 5 eV induces switching of the polarization at the surface.

Electron beam induced switching. We have tracked the kinetics of the e-beam induced switch by recording electron images at 10 frames per second, available in the Supplementary videos. Figure 3 shows a typical image acquired during switching. The field of view (FoV) is 30 μm. Nine domain boundaries (thin horizontal lines) are visible. At t = 0 the SV is switched from 1 to 5 eV. The switching proceeds in a zig-zag pattern around the direction [0$\bar{1}$0]. Domain switching starts from discrete points at an upper domain wall and propagates as rather broad needles until reaching the opposite domain wall. Then, the needles expand until the polarization is switched in the entire domain. In a fourth step, switching then continues in the next

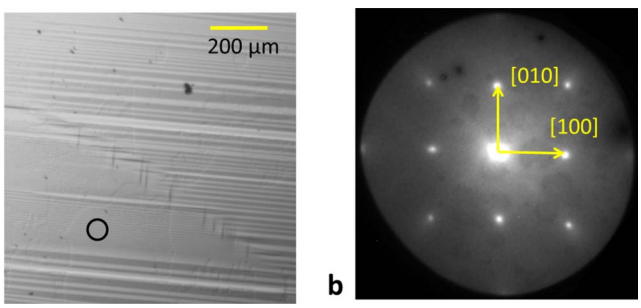

Figure 2 | (a) Optical micrograph of the $BaTiO_3$ surface showing domain ordering on a macroscopic scale. For comparison, the size of the electron beam is indicated by the black circle. (b) (1 × 1) LEED pattern using a primary electron energy of 35 eV.

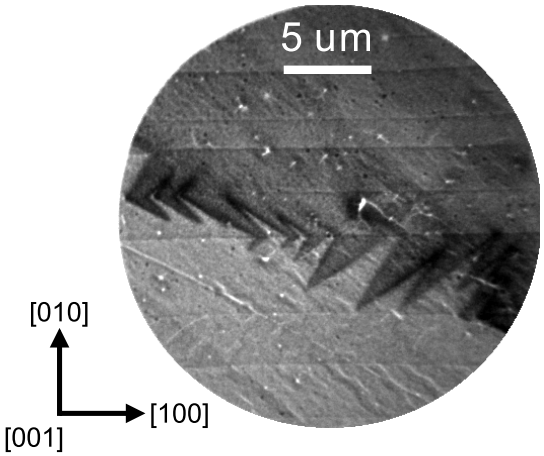

Figure 3 | Electron image of the surface 1.3 seconds after the start voltage has been switched from 1 to 5 eV.

domain but at an angle of 90° with respect to the previous one and so on, until the polarization in the entire field of view has been switched.

An evident contrast variation occurs during the switching process, see Fig. 3. The origin of the contrast observed during the switching is not trivial. The question is whether the domain polarization is in- or out-of-plane, or both. On completion of the switch there is no significant difference in the electron reflectivity between adjacent domains although the overall intensity is slightly lower after the switch. This can be seen from images of the electron reflectivity obtained for SV = 1 eV *before* switching and 5 eV *after* switching in a 30 μm FoV presented in Fig. 4a,b. The sharp horizontal lines are domain walls along [100] and the typical domain width is ~3 μm. Between the switched and the unswitched states the domain walls do not move. Far from the domain walls the intensity is similar showing that surface potential on either side of the wall is the same. This suggests all domains have the same polarization component perpendicular to the surface. The polarization cannot be out-of-plane since domains are visible optically as can be seen in Fig. 2a. Therefore, this strongly suggests that all domains within the field of view have zero polarization perpendicular to the surface and are in fact polarized in-plane. This is confirmed by a close examination of the electron intensity near the domain walls.

Domain walls. As shown in Fig. 1b, a 90° domain wall between two in-plane polarized domains gives rise to an electric dipole perpendicular to the wall. The lateral electric field can, if strong enough with respect to the extractor voltage between sample and objective lens, deviate electrons[27]; consequently, the e-beam is in part cut by the contrast aperture of the LEEM, which determines a change in the image contrast (see discussion for more details). This effect has been used, for instance, to investigate the built-in field at an in-plane p-n junction with low energy photoelectrons[28], however, quantitative evaluation of the dipole strength requires detailed electron optics simulations[27,28].

Fig. 4c shows the normalized intensity profile across the domain wall before switching. The profile obtained across each domain wall is the same (shown in Supplementary Fig. 4). The intensity asymmetry results from the electrons being deflected by the electric field due to the domain wall dipole along $[0\bar{1}0]$. Fig. 4d shows the intensity profiles across the same wall *after* polarization switching. The asymmetry in the intensity profile across the domain wall is reversed, showing that the dipole is now along [010]. The intensity profile across successive domain walls *always* has the same shape, showing that the overall macroscopic polarization is indeed along [010] before and $[0\bar{1}0]$ after switching, see Supplementary Fig. 4. The absence of contrast between adjacent domains and the alignment of the electric domain wall dipoles proves that our domains are in-plane polarized with 90° domain walls. The asymmetry is sharper for the 5 eV electrons, presumably because they interact more closely with the domain wall dipole over a higher penetration depth than the 1 eV electrons. Thus, the low energy electron images not only provide proof that the polarization is in-plane but also show that the switch leaves the ferroelastic domain walls pinned.

Once the switched state is fully attained, the start voltage was then reset to 1 eV and a reverse switch starts immediately, culminating in complete recovery of the original in-plane polarization state. This process is perfectly reproducible. Varying the start voltage between 4.3 and 5.0 eV changes the switching time but the kinetics of needle growth across domains followed by lateral expansion remains identical. Fig. 5 shows the sample bias dependance of the switching time. The switching time decreases with increasing start voltage suggesting that the quantity of injected charge is crucial in switching since 1-R increases with bias, where R is the reflectivity. Below 4.3 eV, no switching is observed whereas at 8.0 eV and above it is below our time resolution (0.1 sec). The back-switching time, on the other hand, remains constant at about 2 seconds. The strong variations in switching time with the start voltage may seem surprising given the changes in reflectivity, for example R = 0.90 (0.87) at 4.0 (5.0) eV. Nevertheless, this represents an injected current variation of 0.6 nA in the elliptical 85–90 μm beam spot. The solid blue line is an exponential fit to the switching time using exp(44.6/SV(eV)). If the injected current plays the role of an applied field switching pulse then this suggests a qualitative agreement with Merz's law. However, the real physical significance of the pre-exponential factor and the activation SV would have to be the subject of a full theoretical and experimental study.

Discussion

Needle domains. With reference to Fig. 1b, the forward needle growth, shown by the thicker, red arrows, followed by lateral expansion provides a minimum energy path for in-plane switching. The electrostatic energy at the needle tip is a high because it is a head-to-head domain wall with positive bound polarization charge. The intensity profile across a needle domain during switching is shown in Fig. 7. It is symmetric, demonstrating that the electric field across the needle domain sidewall is the same on both sides. This corresponds to the formation of head-to-head walls in the polar direction ($[\bar{1}\bar{1}0]$ for the needle highlighted by the profile) and illustrated schematically in Fig. 1b.

The sidewalls, on the other hand, are neutral perpendicular to the direction of needle propagation and therefore have a lower electrostatic energy. The needle-like growth for in-plane switching also minimizes the elastic energy by leaving the tetragonality unchanged. However, when the needle reaches the next domain wall, the electrostatic energy increases because of the positive polarization charge at the original domain wall, temporarily halting the forward propagation and favoring sidewall expansion until the entire domain is switched. Indeed, at an ideal head to head 90° domain wall the surface charge density can be estimated to be 37 μC/cm^2. Furthermore, Gao et al[1] have recently reported that the formation of a glassy electric dipole region at 90° walls stabilizes the wall which would slow down switching. However, the continued arrival of negative injected charge maintaing the head to head configuration finally allows needle growth to proceed in the subsequent domain to reduce the electrostatic energy. One useful analogy for the progression of the needle domains through the ferroelastic wall is that of a zig-zag train of vertically-standing dominoes. Each domino represents the microscopic polarization in a unit cell. Tipping over the first domino provokes a fast forward switching which inevitably slows down going round the corner of the 90° wall, to once again accelerate in the second straight line.

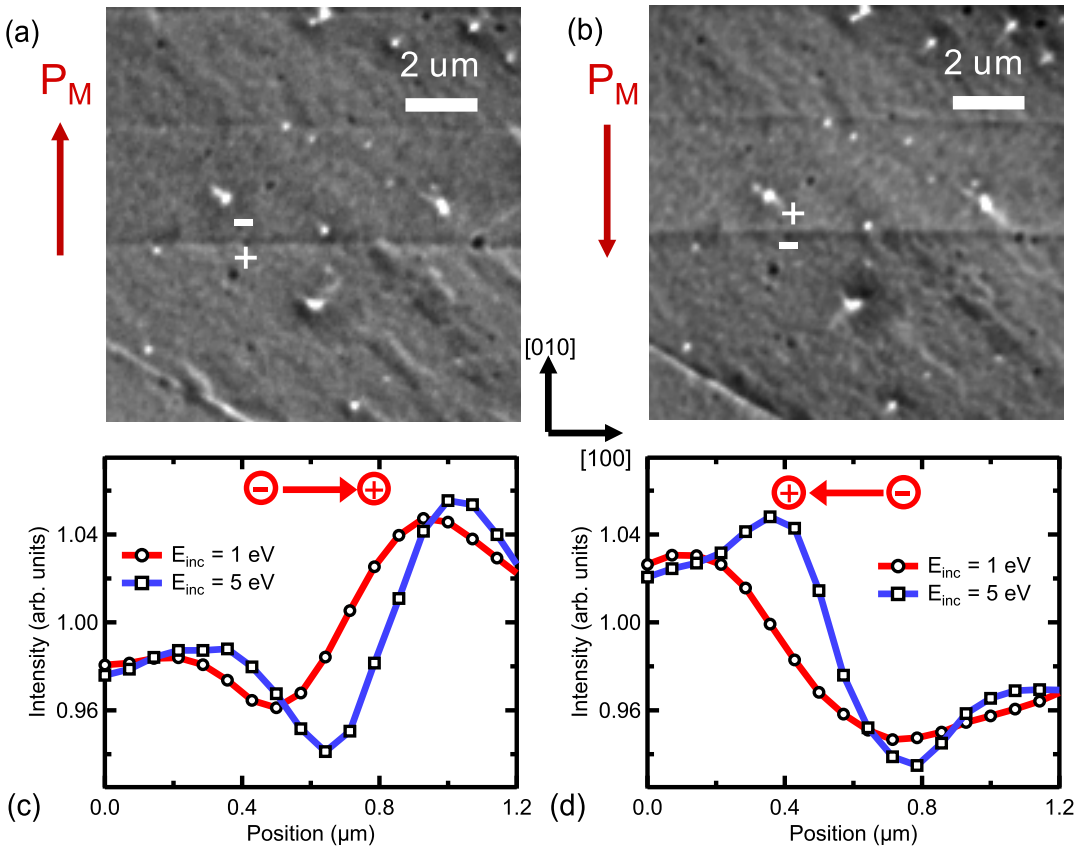

Figure 4 | LEEM images of sample surface before (a) and after (b) switching, the field of view is 30 μm. Intensity profiles extracted from LEEM images acquired using 1 eV (round, red symbols) and 5 eV (square, black symbols) along [0$\bar{1}$0] across a domain wall before (c) and after (d) switching. The deduced electric dipole across the wall is shown by the plus and minus signs.

Switching kinetics. Kinetics of FE switching is usually described in four main stages[29]. Switching starts via nucleation of new domains. Then, these domains grow in the polar direction through the sample (forward growth). During this stage, the domains are often needle-shaped and the domain walls are charged. When the needles reach the counter electrode, the domains grow in the transversal direction of the polar axis via wall motion (sideways domain growth). Finally, the wall motion decelerates and the switching is completed via domain coalescence. The observed switching process follows closely this model.

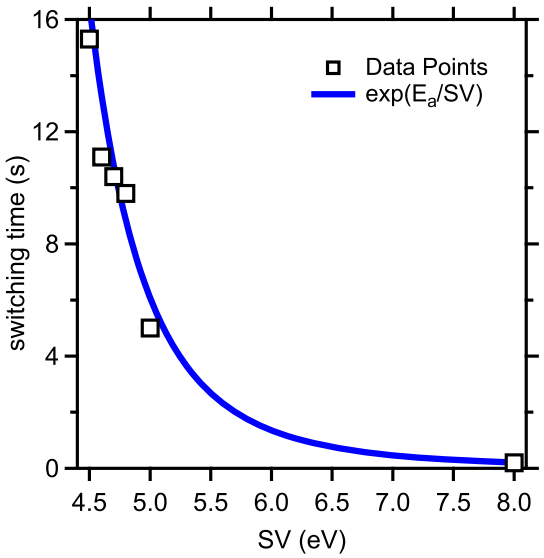

Figure 5 | **Switching time (squares) as a function of sample bias.** Below 4.3 eV the polarization does not switch, at 8 eV the switching is below 0.1 seconds. The blue line is an exponential fit to the data.

Domain nucleation during switching can be modulated by external screening from some kind of electrical circuit and by bulk screening which can have several origins: bound ionic charge, defect dipoles and free screening charge[29], here the incident electrons. The role of bulk screening on domain switching is characterized by τ_{scr}, the screening time constant. High values of τ_{scr} correspond to ineffective bulk screening mechanism, which favors the formation of needle domains during switching. With a macroscopic in-plane polarization before e-beam irradiation along [010], the built-in field to be screened inside each domain is along [1$\bar{1}$0] or [$\bar{1}$1$\bar{0}$]. We suggest the following mechanism for the polarization switch. At a SV of 5 eV electrons penetrate and at a domain wall screen the positive while destabilizing the negative bound charge. The latter are repelled, creating an unstable head-to-head configuration. The local field which results induces further ionic displacements and the head-to-head wall advances. These incremental shifts produce the observed propagation of the needle domain in the forward direction. The process is slow because it depends on fields induced by bound charge displacement and screening of the resulting head-to-head domain walls by the injected electronic charge.

Recent work on in-situ polarization switching has focussed on thin film capacitors[1,2]. Static ferroelastic domain walls and the interaction of applied and built-in fields were shown to play important roles. Here, there is no applied field, however, similar interaction between the polarization switching and ferroelastic domain walls is observed under the injection of low energy electrons.

From Fig. 6, the switched region under the electron beam must result in the formation of head to head domain walls with the sur-

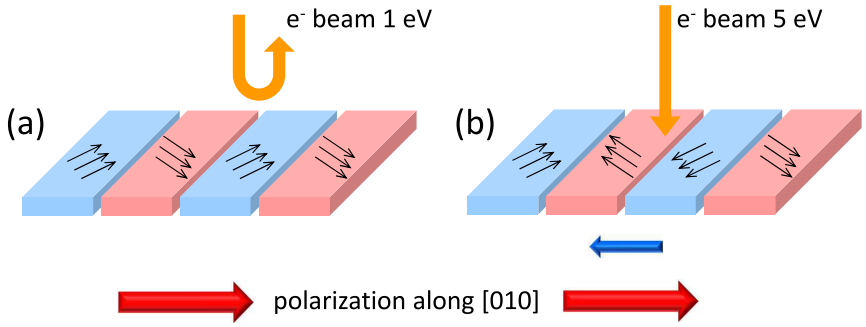

Figure 6 | Schematic of the e-beam induced switching process. Close to the MEM regime (left), electrons are mainly reflected without penetrating the sample surface whereas at higher sample bias (right) injected negative charge alters the screening of domain wall dipoles allowing polarization switching along [0$\bar{1}$0] until the macroscopic polarization points along [010]. The pristine, macroscopic polarization is indicated by the thick (red) horizontal arrow whereas the switched polarization is represented by the thin (blue) horizontal arrow.

rounding unswitched region. These walls are maintained by the continual injection of free charge carriers[30]. When the charge injection is cut off by reducing the bias to 1 eV, the head-to-head configuration is destabilized and the reverse switch sets in from the bottom of the image and moves along [010]. The unscreened macroscopic field due to the pristine, as-received domain structure switches the polarization back to its original direction. The switched state is therefore not a ground state but a steady state resulting from the balance between the equilibrium domain pattern and the injection of negative screening charge.

In a different experiment, Roelofs *et. al.* have studied 180° switching in $PbZr_{0.2}Ti_{0.8}O_3$ films with 90° domain walls[31]. The application of a negative bias to a PFM tip with respect to a bottom electrode gave rise to a similar switch in the domain polarization as seen in cross-section, whilst conserving the 90° domain walls. The authors suggested that the accumulation of bound polarization charge at the domain wall also seeded needle domain growth.

Screening processes including bulk charge, defect dipoles and carrier injection are known to be slow and can be of the order of seconds[29]. In the present experiment, the charge injection switches the polarization at a much slower rate than, for example, a switch activated by the application of an external voltage pulse. The quantity of injected charge varies only slowly with the start voltages used, however the switching time is very sensitive to these variations indicating a delicate balance between screening by injected charge and the macroscopic field of the original domain structure. This also explains why the reverse switch sets in immediately when the incoming electron energy is reduced.

The intensity variation across the needle walls during switching is particularly fascinating. As shown in Fig. 1b the walls are always head-to-head in the polar direction. The advancing front of the needle domains has therefore bound positive charge which in the LEEM experiment modifies local surface potential[30] increasing the effective electron kinetic energy. As a result the reflectivity R decreases and the needle front appears dark in the electron images. Perpendicular to the sidewalls there is little or no excess bound charge, however, along the sidewall, at the apex of each arrow in Fig. 1b, there must be head to head (positive charge) configurations, responsible for the lower intensity observed on the sidewalls, observed in Fig. 7b.

However, we must also account for the significant contrast between the switched and unswitched regions during the switching process. We argue that this contrast arises due to a different electron beam deflection caused by the in-plane electric field, similar to Lorentz microscopy. The alignment conditions were optimized to image complete domains on the sample before switching. On switching, the optimum imaging conditions will change, but the microscope settings do not. In other words, the electrons reflected from the switched part of the surface are slightly deviated from the optical axis, whose alignment was set before switching. This can be seen by comparison of images taken without and with an aperture inserted into the back focal plane of the microscope, shown in the Supplementary Fig. 6. In the back focal plane electrons with higher take-off angles with respect to the sample normal are further from the optical axis. The insertion of an aperture results in strongly deviated electrons being cut off and the contrast between switched and unswitched domains increases.

Following these arguments one would expect that irradiating a sample with positive charge should induce the reverse switching effect. From symmetry, the same effect could be obtained by rotating

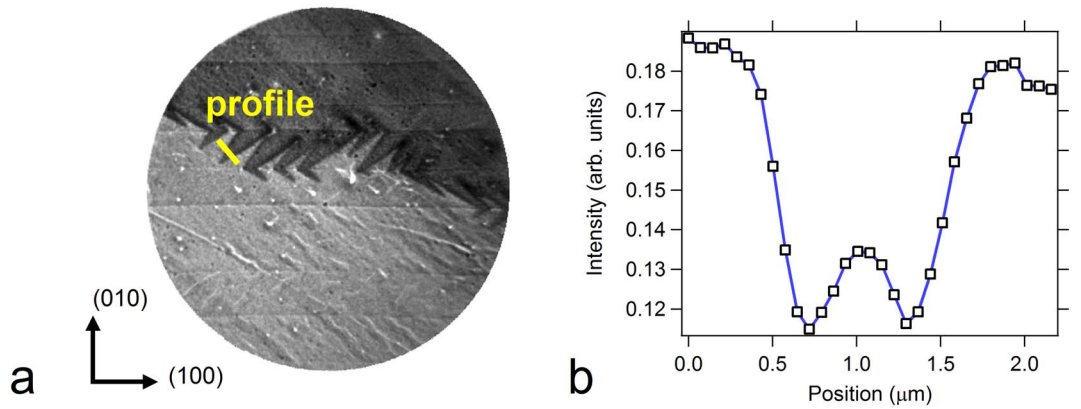

Figure 7 | (a) Electron image of $BaTiO_3$ surface during switching, the thick yellow line shows where the intensity profile was taken (b) Intensity profile across needle domain perpendicular to the polar direction.

the sample 180° around the normal and using the low energy electron beam, however, this is not yet possible in our experiment.

We have shown that a very low energy electron beam can reversibly switch in-plane polarization of single crystal $BaTiO_3$. Using a low energy electron microscope we can simultaneously switch and image the in-plane domain polarization. Switching proceeds by propagation of needle domains along the polar direction and then sidewall expansion to complete the polarization switch within the domain. We suggest that the injected charge destabilizes the polarization charge at domain walls, switching the polarization whilst preserving the ferroelastic domain pattern. The current density required to switch the in-plane polarization is 0.26 mA/cm^2. This scales to 1 pA for a 10 μm long domain of the same width (3 μm) as in our experiment. Tuning the electron energy allows to increase the switching speed by orders of magnitude. One could imagine low power opto-electronic devices based on such phenomena.

Methods

Low energy electron microscopy. Our experiments have been carried out using a spectroscopic photoemission and low energy electron microscope (SPELEEM) in the low energy (negative charging) range. The electron gun emits electrons at 18 kV which are then decelerated by the sample bias to very low electron kinetic energy (KE). The reflected and backscattered electrons are then imaged using a cathode, or immersion, lens system in which the electrons are reaccelerated by by the same bias voltage between the sample and the objective lens. To limit aberrations and therefore improve lateral resolution, an angle-limiting aperture, called the contrast aperture, can be inserted into the back focal plane of the objective lens, reducing the spherical and chromatic aberrations. Additional lenses are then used for the electron-optical magnification and images are recorded using a double multichannel plate and fluorescent screen. The exact incident electron energy is tuned using a variable part of the sample bias (the so-called start voltage) over a few eV.

At very low KE, called mirror electron microscopy (MEM), electrons are reflected without penetrating the sample surface. The local reflectivity is a measure of the local work function of the specimen, which is determined by different factors such as composition, morphology etc. In this way, the surface charge and hence polarization can be estimated[18]. At higher bias voltages (LEEM), the electrons penetrate the surface. While part of the beam is elastically backscattered, the rest results in the accumulation of charge within the topmost layers. Above ~10 eV, secondary electrons are generated and collective excitations such as plasmons become significant[32], giving rise to variations in the elastic peak intensity. In this energy range, the electron inelastic mean free path is of the order of 1 nm. However, in the intermediate regime between MEM and LEEM (below ~5–10 eV), called Very low electron microscopy (VLEEM)[33,34], the electron wavelength is considerably greater than the atomic spacing making it too large for crystalline diffraction. The energy is also too low for significant inelastic losses due to plasmon excitations and scattering from interaction with band structure of the material increases. In this regime, the main source of inelastic losses are individual electron excitation to allowed states above the Fermi level and electron-phonon interactions[33]. As a result, the inelastic mean free path increases significantly[26] and electrons penetrate several tens of nm into the sample.

The base pressure in the SPELEEM set-up was 2×10^{-8} Pa. In the illumination column the electrons are accelerated to 18 kV and are decelerated just before the sample. The band width is ~0.5 eV. The reflected electrons are then reaccelerated to 18 kV for imaging using a double multichannel plate and video camera. The electron optics of the SPELEEM provides a highly collimated monochromatic beam with a spatial resolution of 12 nm. The electron energy is defined in terms of the start voltage, which is measured with respect to the LaB_6 cathode work function. Incident electron kinetic energy is controlled by changing the sample bias. The photoelectron emission micrcoscopy data was acquired using the same microscope and synchrotron radiation. A 20 μm iris aperture in an intermediate image plane ensured that the photoemission spectra were recorded from the centre of the field of view used in LEEM. All raw images were divided by a flat field obtained out of focus far below the MEM-LEEM transition in order to eliminate detector defects.

1. Gao, P. *et al.* Atomic-scale mechanisms of ferroelastic domain-wall-mediated ferroelectric switching. *Nature Comm.* **4**, 2791 (2013).
2. Lee, J. K. *et al.* Direct observation of asymmetric domain wall motion in a ferroelectric capacitor. *Acta Materialia* **61**, 6765–6777 (2013).
3. Merz, W. J. Domain formation and domain wall motions in ferroelectric $BaTiO_3$ single crystals. *Phys. Rev.* **95** (1954).
4. Li, D. B., Strachan, D. R., Ferris, J. H. & Bonnell, D. A. Polarization reorientation in ferroelectric lead zirconate titanate thin films with electron beams. *J. Mat. Research* **21**, 935–940 (2006).
5. Ferris, J. H., Li, D. B., Kalinin, S. V. & Bonnell, D. A. Nanoscale domain patterning of lead zirconate titanate materials using electron beams. *Appl. Phys. Lett.* **84**, 774 (2004).
6. Ng, N., Ahluwalia, R. & Srolovitz, D. J. Depletion-layer-induced size effects in ferroelectric thin films: A Ginzburg-Landau model study. *Phys. Rev. B* **86**, 094104 (2012).
7. Ahluwalia, R. *et al.* Manipulating ferroelectric domains in nanostructures under electron beams. *Phys. Rev. Lett.* **111**, 165702 (2013).
8. Li, D. & Bonnell, D. A. Controlled patterning of ferroelectric domains: fundamental concepts and applications. *Ann. Rev. Mater. Res.* **38**, 351–368 (2008).
9. Yakshinskiy, B. V., Hedhili, M. N., Zalkind, S., Chandhok, M. & Madey, T. E. Radiation-induced defect formation and reactivity of model TiO_2 capping layers with MMA: a comparison with Ru *Emerging Lithographic Technologies Xii, Pts 1 and 2* **6921**, 692114–692114–10 (2008).
10. Jia, C.-L. *et al.* Atomic-scale study of electric dipoles near charged and uncharged domain walls in ferroelectric films. *Nature Mat.* **7**, 57–61 (2008).
11. Gao, P. *et al.* Revealing the role of defects in ferroelectric switching with atomic resolution. *Nature Comm.* **2**, 591 (2011).
12. Nelson, C. T. *et al.* Domain dynamics during ferroelectric switching. *Science* **334**, 968–971 (2011).
13. Gruverman, A., Wu, D. & Scott, J. F. Piezoresponse force microscopy studies of switching behavior of ferroelectric capacitors on a 100-ns time scale. *Phys. Rev. Lett.* **100** (2008).
14. Kim, T. H. *et al.* Polarity-dependent kinetics of ferroelectric switching in epitaxial $BiFeO_3$ capacitors. *Appl. Phys. Lett.* **99** (2011).
15. Barrett, N. *et al.* Full field electron spectromicroscopy applied to ferroelectric materials. *J. Appl. Phys.* **113**, 187217 (2013).
16. Cherifi, S. *et al.* Imaging ferroelectric domains in multiferroics using a low-energy electron microscope in the mirror operation mode. *phys. stat. sol. (RRL)* **4**, 22–24 (2010).
17. Wang, J. L., Vilquin, B. & Barrett, N. Screening of ferroelectric domains on $BaTiO_3$(001) surface by ultraviolet photoinduced charge and dissociative water adsorption. *Appl. Phys. Lett.* **101**, 092902 (2012).
18. Rault, J. *et al.* Thickness-dependent polarization of strained $BiFeO_3$ films with constant tetragonality. *Phys. Rev. Lett.* **109**, 267601 (2012).
19. Cochran, W. Crystal stability and the theory of ferroelectricity. *Adv. Phys.* **9**, 387–423 (1960).
20. Hwang, J., Kolodiazhnyi, T., Yang, J. & Couillard, M. Doping and temperature-dependent optical properties of oxygen-reduced $BaTiO_{3-\delta}$. *Phys. Rev. B* **82**, 214109 (2010).
21. Iwazaki, Y., Suzuki, T., Mizuno, Y. & Tsuneyuki, S. Doping-induced phase transitions in ferroelectric $BaTiO_3$ from first-principles calculations. *Phys. Rev. B* **86**, 214103 (2012).
22. Rault, J. E. *et al.* Polarization sensitive surface band structure of doped $BaTiO_3$(001). *Phys. Rev. Lett.* **111**, 127602 (2013).
23. Hirata, A., Ando, A., Saiki, K. & Koma, A. Characterization of surface defects formation in strontium titanate (100). *Surf. Sci.* **310**, 89–94 (1994).
24. Kuwabara, M., Matsuda, H. & Hamamotot, K. Differential negative resistance and piezoresistivity in thin semiconducting batio ceramic bars. *J. Am. Ceram. Soc.* **80**, 1881–1884 (1997).
25. Kessel, M., De Souza, R. A., Yoo, H.-I. & Martin, M. Strongly enhanced incorporation of oxygen into barium titanate based multilayer ceramic capacitors using water vapor. *Appl. Phys. Lett.* **97**, 021910 (2010).
26. Ziaja, B., London, R. A. & Hajdu, J. Ionization by impact electrons in solids: Electron mean free path fitted over a wide energy range. *J. Appl. Phys.* **99**, 033514 (2006).
27. Nepijko, S. A., Sedov, N. N. & Schönhense, G. Peculiarities of imaging one- and two-dimensional structures using an electron microscope in the mirror operation mode. *Journal of Microscopy* **203**, 269–276 LA – en (2001).
28. Lavayssière, M., Escher, M., Renault, O., Mariolle, D. & Barrett, N. Electrical and physical topography in energy-filtered photoelectron emission microscopy of two-dimensional silicon pn junctions. *Journal of Electron Spectroscopy and Related Phenomena* **186**, 30–38 (2013).
29. Shur, V. Y. Kinetics of ferroelectric domains: Application of general approach to $LiNbO_3$ and $LiTaO_3$. *J. Mat. Sci.* **41**, 199–210 (2006).
30. Zuo, Y., Genenko, Y. A., Klein, A., Stein, P. & Xu, B. Domain wall stability in ferroelectrics with space charges. *J. Appl. Phys.* **115**, 084110 (2014).
31. Roelofs, A. *et al.* Depolarizing-field-mediated 180° switching in ferroelectric thin films with 90° domains. *Appl. Phys. Lett.* **80**, 1424 (2002).
32. Tromp, R. M. *et al.* A simple energy filter for low energy electron microscopy/photoelectron emission microscopy instruments. *J. Phys. Condens. Matter* **21**, 314007 (2009).
33. Cazaux, J. Reflectivity of very low energy electrons (¡ 10 eV) from solid surfaces: Physical and instrumental aspects. *J. Appl. Phys.* **111**, 064903 (2012).
34. Frank, L. & Müllerová, I. The injected-charge contrast mechanism in scanned imaging of doped semiconductors by very slow electrons. *Ultramicroscopy* **106**, 28–36 (2005).

Acknowledgments

J.E.R. was funded by CEA Ph.D. grants and by the Labex PALM APTCOM project. We thank ELETTRA (Trieste) for provision of synchrotron radiation facilities. We gratefully

acknowledge funding from the Agence National de la Recherche project ANR-12-IS04-0001-01 CHEM-SWITCH.

Author contribution

N.B. organized and initiated the project. O.M and A.L. ran the electron microscope and the PEEM facilities. All authors did the experiments. J.E.R. analyzed the data. All authors participated in the preparation of the manuscript.

Additional information

Supplementary Information accompanies this paper at http://www.nature.com/scientificreports

Competing financial interests: The authors declare no competing financial interests.

How to cite this article: Rault, J.E., Menteş, T.O., Locatelli, A. & Barrett, N. Reversible switching of in-plane polarized ferroelectric domains in $BaTiO_3$(001) with very low energy electrons. *Sci. Rep.* **4**, 6792; DOI:10.1038/srep06792 (2014).